RESEARCH ARTICLE

Global Change Biology **WILEY**

Assessing the impacts of past and ongoing deforestation on rainfall patterns in South America

Confidence Duku[1,2] | Lars Hein[2]

[1]Wageningen Environmental Research, Climate Resilience Team, Wageningen University & Research, Wageningen, the Netherlands

[2]Environmental Systems Analysis Group, Wageningen University, Wageningen, the Netherlands

Correspondence
Confidence Duku, Wageningen Environmental Research, Climate Resilience Team, Wageningen University & Research, P.O. Box 47, 6700 HB Wageningen, the Netherlands.
Email: confidence.duku@wur.nl

Abstract

Despite recent advances in modeling forest–rainfall relationships, the current understanding of changes in observed rainfall patterns resulting from historical deforestation remains limited. To address this knowledge gap, we analyzed how 40 years of deforestation has altered rainfall patterns in South America as well as how current Amazonian forest cover sustains rainfall. First, we develop a spatiotemporal neural network model to simulate rainfall as a function of vegetation and climate inputs in South America; second, we assess the rainfall effects of observed deforestation in South America during the periods 1982–2020 and 2000–2020; third, we assess the potential rainfall changes in the Amazon biome under two deforestation scenarios. We find that, on average, cumulative deforestation in South America from 1982 to 2020 has reduced rainfall over the period 2016–2020 by 18% over deforested areas, and by 9% over non-deforested areas across South America. We also find that more recent deforestation, that is, from 2000 to 2020, has reduced rainfall over the period 2016–2020 by 10% over deforested areas and by 5% over non-deforested areas. Deforestation between 1982 and 2020 has led to a doubling in the area experiencing a minimum dry season of 4 months in the Amazon biome. Similarly, in the Cerrado region, there has been a corresponding doubling in the area with a minimum dry season of 7 months. These changes are compared to a hypothetical scenario where no deforestation occurred. Complete conversion of all Amazon forest land outside protected areas would reduce average annual rainfall in the Amazon by 36% and complete deforestation of all forest cover including protected areas would reduce average annual rainfall in the Amazon by 68%. Our findings emphasize the urgent need for effective conservation measures to safeguard both forest ecosystems and sustainable agricultural practices.

KEYWORDS
Amazon, Cerrado, deforestation, machine learning, rainfall

1 | INTRODUCTION

The crucial role of forests in maintaining rainfall patterns is increasingly evident, with deforestation being a significant driver that affects rainfall patterns at local, regional, and global scales (Cui et al., 2022; Lawrence & Vandecar, 2015; Meier et al., 2021; Smith et al., 2023; Spracklen & Garcia-Carreras, 2015; te Wierik et al., 2021). With global water availability increasingly affected by climate change (Konapala et al., 2020; Masson-Delmotte et al., 2021), understanding the mechanisms by which forests maintain rainfall patterns is becoming more

critical. In recent decades, numerous studies, particularly in the Amazon, have greatly improved our understanding of how deforestation leads to changes in rainfall patterns (e.g., Salazar et al., 2015; Spracklen & Garcia-Carreras, 2015; Staal, Flores, et al., 2020). These studies were partly motivated by the ongoing forest loss in South America especially in Brazil (Amigo, 2020; Kalamandeen et al., 2018; Souza et al., 2020). For example, Brazil has lost an estimated 50 million hectares (11.3%) of the Amazon rainforest and 27.5 million hectares (20%) of native vegetation in the Cerrado between 1985 and 2021 (Curtis et al., 2018; Souza et al., 2020). While these studies are useful for understanding the mechanisms by which large-scale deforestation affects rainfall patterns, they do not necessarily reflect the complexity of real-world deforestation processes and their cumulative effects over time especially at the continental scale. However, there are a few notable studies, such as Khanna et al. (2017), that have captured the relationship between small-scale deforestation and changes in rainfall patterns at the subnational scale.

In this study, we analyze the cumulative impacts of historical deforestation (i.e., between 1982 and 2020) on rainfall patterns across South America. We pay particular attention to capturing both local and remote effects to provide a broader picture of the complex interactions between deforestation and rainfall patterns, accounting for the diverse range of deforestation processes and their spatiotemporal dynamics. Specifically, we assess the spatial impacts of deforestation on various aspects of rainfall, including magnitude, relative entropy, dry season length, and dry season intensity. Furthermore, we project the potential effects of future deforestation on rainfall patterns both inside and outside protected areas in the Amazon biome, given the high vulnerability of unprotected areas to land-use conversion. To accomplish this, we utilize a spatiotemporal neural network modeling approach to capture spatial patterns and dependencies between grid cells, as well as recurrent connections to capture temporal patterns and dependencies between grid cells over time. We analyze the effects of different types of past deforestation, such as commodity-driven deforestation (CDD) and shifting agriculture-driven deforestation (SAG), to provide a more nuanced understanding of the problem. This study builds upon and enhances a previously deployed data-driven modeling approach that used input data from Sub-Saharan Africa (Duku & Hein, 2021).

2 | METHODOLOGY

Our methodology consists of three steps: (i) development of a spatiotemporal neural network model, that we name 'DeepRainForest', which predicts daily rainfall as a function of climate and vegetation inputs; (ii) assessment of the effects of historical deforestation during the periods 1982–2020 and 2000–2020 on rainfall patterns; and (iii) prediction of potential rainfall changes assuming deforestation continues in the Amazon biome. By analyzing the effects of past deforestation on rainfall in two time periods, we are able to disentangle the effects of recent deforestation (i.e., 2000–2020) from the effects of long-term deforestation (i.e., 1982–2020).

2.1 | Developing the DeepRainForest model

We developed the DeepRainForest model to predict daily rainfall across South America as a function of daily wind speed and direction, air pressure on the surface of the earth (ERA5 Reanalysis, Hersbach et al. (2020)), sea-surface temperature (Reynolds & Banzon, 2008), fractional tree and herbaceous cover (DiMiceli et al., 2021), leaf area index (LAI; Myneni et al., 2015), and black sky albedo for the near infrared broadband (Schaaf & Wang, 2015). The selection of these variables was based on an extensive review of the existing literature (e.g., Ellison et al., 2017; Spracklen et al., 2018). We obtained all climate data from reanalysis sources (ERA5 Reanalysis, Hersbach et al. (2020)) at a spatial resolution of 0.25 decimal degrees. Reanalysis data provide a comprehensive and consistent dataset that combines various observations and models to reconstruct past climate conditions and are widely used to understand the forest–rainfall relationship (e.g., Staal et al., 2018; Staal, Fetzer, et al., 2020). In addition, vegetation data were acquired from satellite measurements (DiMiceli et al., 2021; Myneni et al., 2015; Schaaf & Wang, 2015).

To align the spatiotemporal resolutions of climate and vegetation data, tree cover, herbaceous cover, and LAI data were temporally downscaled to daily time-steps using Fast Fourier transform (Virtanen et al., 2020). All vegetation data were then regridded to 0.25 decimal degrees to align with the spatial resolution of climate data. The DeepRainForest model is based on the Convolutional Long-Short Term Memory (ConvLSTM) neural network. The ConvLSTM is a type of recurrent neural network, which has the capacity to learn long-term dependencies between response and predictor variables and preserve the three-dimensional structure of spatiotemporal data sequences (Shi et al., 2015).

ConvLSTM layers, like LSTMs, consist of memory cells and three self-parameterized gates that regulate information flow. Equations (1–6) provide a general description of a ConvLSTM layer according to (Xingjian et al., 2015). Memory cells, represented as C_t, gather information from input data over extended periods of time. The forget gate, f_t, decides which information should be discarded from the previous cell state, C_{t-1}. The input gate, i_t, in conjunction with a tanh layer, g_t, updates the previous cell state. The input gate determines which information from the previous cell state, C_{t-1}, should be updated, while the tanh layer decides which candidate information from the current input data, X_t, and the previous output/hidden state, H_{t-1}, should be added to the memory cell. The output gate, o_t, determines which information from the current cell state, C_t, should be propagated to the current hidden state, H_t, and therefore, become a candidate for accumulation in the cell state during the next sequence. The input, forget, and output gates are made up of sigmoid functions, σ, with values ranging from 0 to 1, that regulate the amount of information passing through the gates. For instance, if f_t equals 0, the model discards all information stored in the previous cell state, and if it equals 1, it retains all previous information. W represents the weight, which indicates the strength of connection between units in each layer, and b is the bias, which is similar to a

constant in a linear function. The symbol ⊙ represents an element-wise dot product, and * indicates the convolution operator.

$$i_t = \sigma\left(W_{i\_xi} * X_t + W_{i\_hi} * H_{t-1} + W_{i\_ci} \odot C_{t-1} + b_i\right), \quad (1)$$

$$f_t = \sigma\left(W_{f\_xf} * X_t + W_{f\_hf} * H_{t-1} + W_{f\_cf} \odot C_{t-1} + b_f\right), \quad (2)$$

$$o_t = \sigma\left(W_{o\_xo} * X_t + W_{o\_ho} * H_{t-1} + W_{o\_co} \odot C_t + b_o\right), \quad (3)$$

$$g_t = \tanh\left(W_{g\_xc} * X_t + W_{g\_hc} * H_{t-1} + b_c\right), \quad (4)$$

$$C_t = f_t \odot C_{t-1} + i_t \odot g_t, \quad (5)$$

$$H_t = o_t \odot \tanh(C_t). \quad (6)$$

The DeepRainForest network architecture consists of four stacked ConvLSTM layers, which are interposed between two stacked convolutional layers and two stacked transposed convolutional layers. The presented architecture allows for capturing local and remote effects of vegetation changes on rainfall by utilizing convolutional filters to capture spatial patterns and dependencies between grid cells, as well as recurrent connections to capture temporal patterns and dependencies over time. The stacking of multiple layers of convolutional filters in the network architecture, allows the network to capture spatial dependencies at multiple scales. The detailed neural network architecture is presented in Figure S1. This current version is an enhancement of a model that we previously deployed across Sub-Saharan Africa (Duku & Hein, 2021). Compared to the prior version, this current version operates at a higher spatial resolution (i.e., 0.25 decimal degrees), incorporates additional vegetation data (i.e., albedo and fractional herbaceous cover) and adds sea-surface temperature data. Sea-surface temperature in the Atlantic and Pacific oceans are strong modulators of the regional climate in South America influencing weather patterns, precipitation, and atmospheric circulation. Albedo represents the reflectivity of land surfaces and plays a crucial role in the energy balance and feedback processes within the Earth's climate system.

The DeepRainForest model was trained on daily time series of input data and ERA5 rainfall data (Hersbach et al., 2020) from 2001 to 2013 and evaluated on an independent test sample from 2014 to 2018. A variety of pairwise comparison statistics were employed to evaluate the predictive accuracy of the model at both daily and monthly time-steps. Four statistical indicators were computed for the pairwise comparison statistics. They included the Nash–Sutcliffe efficiency (NSE), Kendall tau correlation coefficient, root mean squared error (RMSE), and percentage bias (PBIAS).

2.2 | Quantifying the impacts of past and future deforestation on rainfall

To investigate the impact of historical deforestation on rainfall patterns, specifically focusing on CDD and SAG, we identified deforestation hotspots (Figure 1) associated with these drivers based on
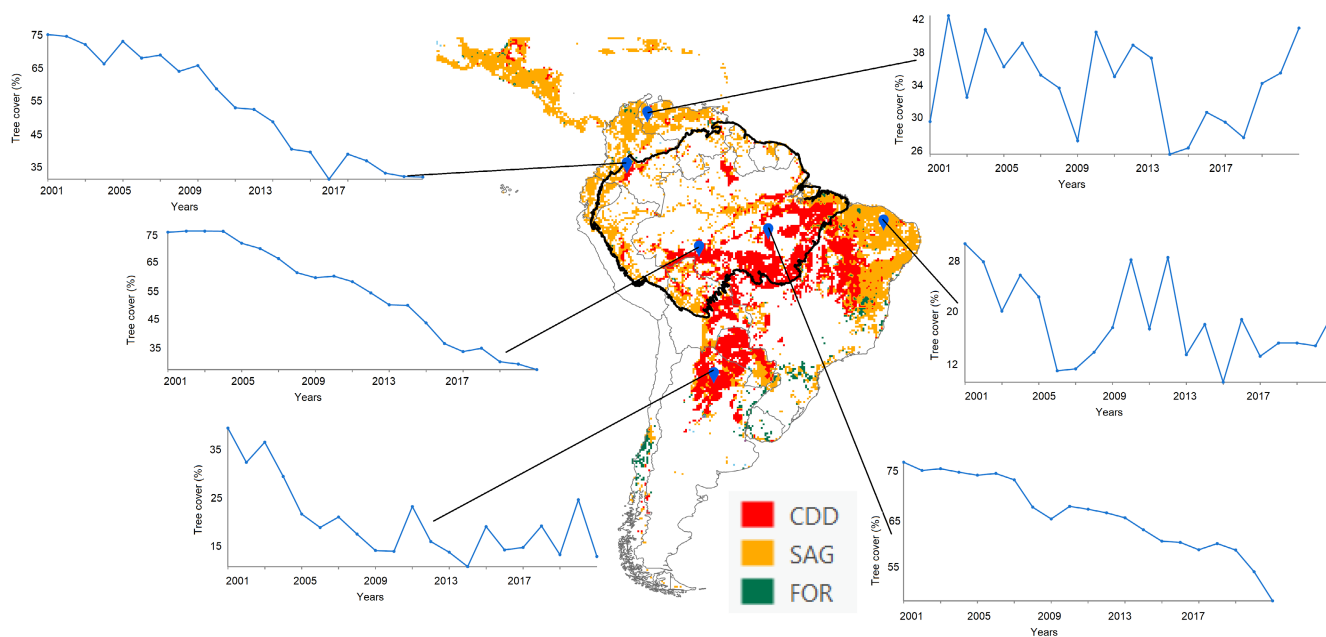

FIGURE 1 Deforestation hotspots and their underlying drivers, adapted from Curtis et al. (2018). All colored areas are deforestation hotspots between 2001 and 2015, categorized as follows: Commodity-driven deforestation (CDD) which represents areas where forest loss and deforestation are driven by commodity production characterized by long-term, permanent conversion of forest and shrubland to a non-forest land use such as agriculture; shifting agriculture (SAG) which represents areas where forest loss is driven by small- to medium-scale forest and shrubland conversion for agriculture that is later abandoned and followed by subsequent forest regrowth; forestry (FOR) which represents areas where forest loss is driven by large-scale forestry operations occurring within managed forests and tree plantations with evidence of forest regrowth in subsequent years. For each indicated point, the time-series subplots depict the tree cover from 2001 to 2020.

data from Curtis et al. (2018) and performed controlled simulations by maintaining tree cover and vegetation data in these hotspots constant at 1982 and 2000 levels. The data from Curtis et al. (2018) represent aggregated forest loss occurrences with attribution to specific drivers. However, it is important to note that these data do not account for medium- to long-term forest cover dynamics. As a result, areas with a generally increasing forest cover trend, despite few instances of recorded forest loss, were also included in the delineated deforestation zones. For our analysis, we did not consider such areas as hotspots of forest loss. To eliminate such areas from the data, we tested annual tree cover data between 2001 and 2020 for trends using Mann Kendall trend test. Grid cells that had been designated as deforestation hotspots by Curtis et al. (2018) and that overlapped with areas with statistically significant ($p < .1$) positive trend in tree cover were then eliminated and not used in our analysis.

Several control simulations were conducted, each of which involved holding tree cover, non-tree vegetation cover, LAI and albedo constant at 1982 and 2000 levels in the delineated hotspots (i.e., CDD, SAG, and the areas of both CDD and SAG) throughout the simulation period. For all control simulations, all climate input data remained unchanged from simulation with actual deforestation. Vegetation data outside the delineated deforestation hotspots also remained unchanged. As input to the control simulations, LAI and albedo time-series data for 1982–2000 were computed by deriving typical year-round LAI and albedo profiles for different tree cover intervals (e.g., 75%–80% tree cover) (Figure 2). For each tree cover interval, the LAI and albedo profiles are based on the day-of-year average for the period 2001–2020.

For all simulations, that is, with and without historical deforestation, we computed and compared the rainfall magnitude, relative entropy, dry season length, and dry season intensity. Rainfall magnitude is the annual rainfall total. Relative entropy is a threshold-independent information theory measure that quantifies the extent of annual rainfall concentration (Feng et al., 2013). It ranges from 0 to 3.6, with a value of 0 indicating uniform monthly rainfall

distribution throughout the year and 3.6 indicating that annual rainfall is concentrated in only 1 month. Dry season length is the number of months where mean monthly rainfall is less than mean monthly potential evapotranspiration (Aragão et al., 2007). Monthly estimates of potential evapotranspiration were obtained from Abatzoglou et al. (2018). The original dataset was at a spatial resolution of 2.5 arc-minute and was subsequently regridded to 0.25 decimal degrees. The potential evapotranspiration was computed using the Penman Montieth approach (Allen et al., 1998). Dry season intensity is the total cumulative water deficit during dry months (Aragão et al., 2007). Rainfall magnitude, R_k; relative entropy, D_k; dry season length, DSL; and dry season intensity, DSI, were calculated using Equations (7–11), where the associated monthly rainfall distribution, $p_{k,m}$, and the relative entropy, D_k are computed from the monthly total rainfall $r_{k,m}$ and where q_m is the uniform distribution, for which each month has a value of 1/12; m is the number of months in the year; p_m is the mean monthly rainfall for month m; and PET_m is the mean monthly potential evapotranspiration for month m.

$$R_k = \sum_{m=1}^{12} r_{k,m}, \tag{7}$$

$$p_{k,m} = \frac{r_{k,m}}{R_k}, \tag{8}$$

$$D_k = \sum_{m=1}^{12} p_{k,m} \log_2\left(\frac{p_{k,m}}{q_m}\right), \tag{9}$$

$$DSL = \left[m: \sum (p_m - PET_m) \right], \tag{10}$$

$$DSI = \sum (PET_m - P_m). \tag{11}$$

To better understand the relation between forest cover and rainfall in the Amazon biome, we conducted two additional assessments. First, we examined the effects of complete tree cover loss outside
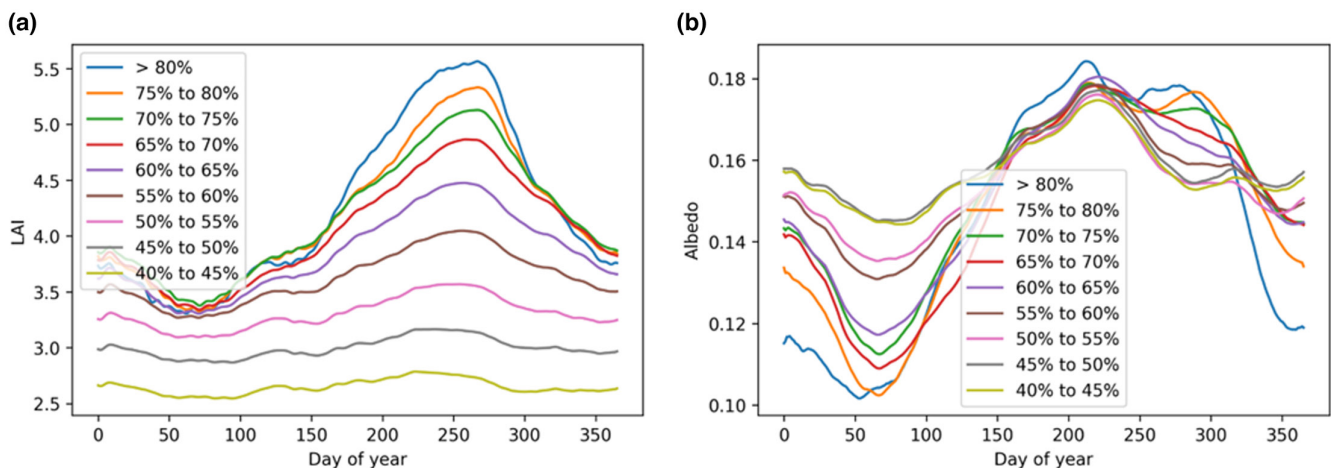

FIGURE 2 Leaf area index (LAI) (a) and albedo (b) profiles used as input for the control simulations. LAI and albedo profiles were derived for different tree cover intervals based on data from 2001 to 2020.

of protected areas (Figure S2), which would be a rather extreme, but not entirely unthinkable scenario for future tree cover decline. Data from UNEP-WCMC and IUCN (2022) were used to delineate the protected areas (Figure S2). Second, we looked at the impact of complete tree cover loss in the entire Amazon biome in order to illustrate the overall importance of forest cover for maintaining rainfall patterns. As inputs to our partial and complete deforestation simulations, the LAI and albedo profiles of each respective tree cover scenario were derived following the approach earlier described in this section (Figure 2).

3 | RESULTS

3.1 | DeepRainForest model performance assessment

Our model is able to reproduce the spatiotemporal pattern of rainfall with high accuracy (Figure 3). On a daily time-step, the DeepRainForest model (Figure 4) achieves NSE and Kendall tau correlation coefficients greater than 0.5 over large areas especially over forested regions such as the Brazilian Amazon, Mata Atlantica, the
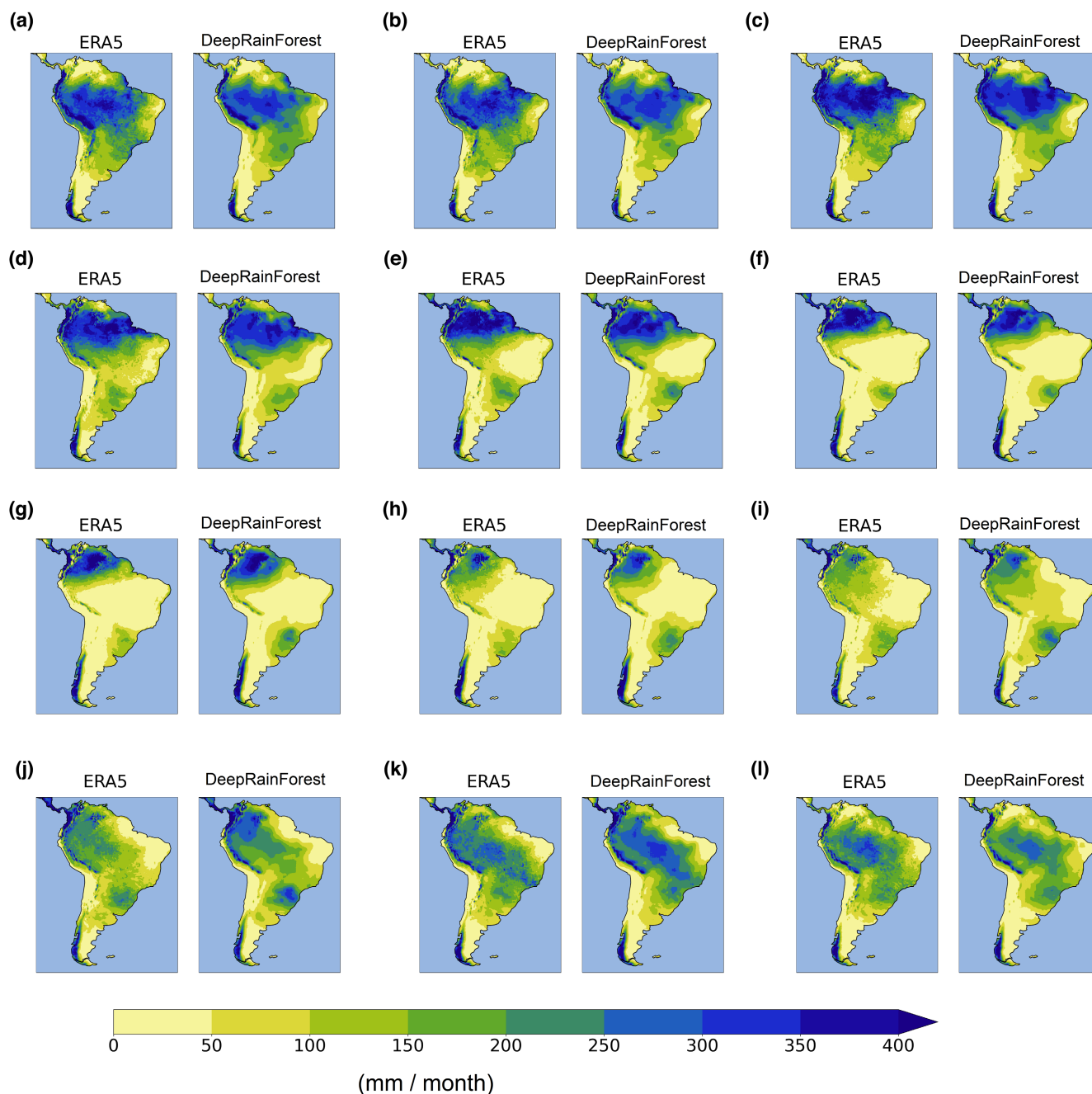

FIGURE 3 Comparison of observed (ERA5) and mean monthly spatial rainfall patterns predicted by DeepRainForest from January (a) to December (l) over the validation period, that is, 2014–2018.
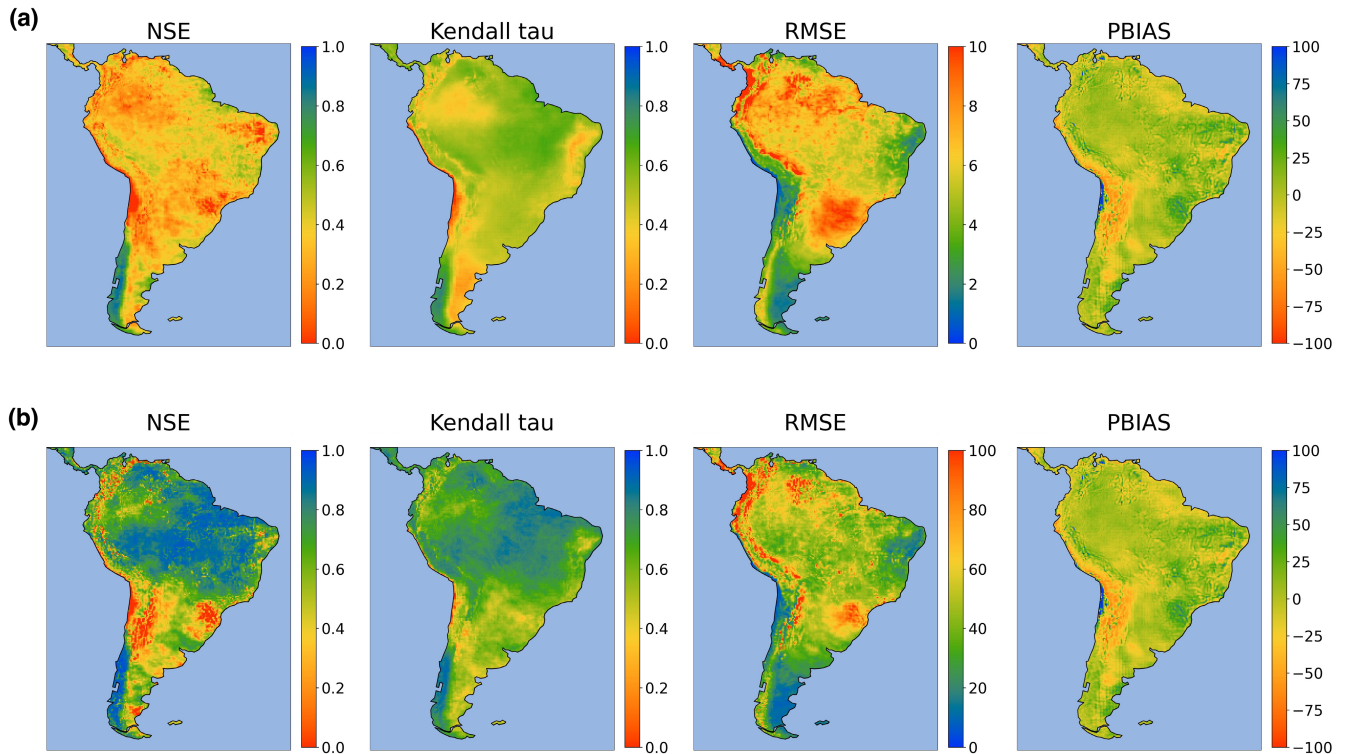
FIGURE 4 DeepRainForest model performance metrics at daily time-step (a) and monthly time-step (b). NSE is Nash–Sutcliffe efficiency and higher values indicate greater accuracy. Higher values for Kendall tau also indicate greater correlation between observed and predicted rainfall. RMSE is root mean squared error and lower values indicate less predictive error. PBIAS is percent bias and negative values indicate model underestimation whereas positive values indicate overestimation. The metrics were computed based on ERA5 and simulated rainfall data in the validation period, that is, 2014–2018.

Chilean temperate forest areas as well as the Cerrado region (4a). For monthly time-step, the NSE and Kendall tau coefficients increase substantially over the aforementioned forested regions and the Cerrado to over 0.75 (4b), indicating the accuracy of our model for several biomes. Over these areas the model on average tends to overestimate both daily and monthly rainfall prediction. This can be attributed to the high frequency of dry days, that is, days with 0 mm of rainfall. For a substantial portion of these days, our model tends to predict rainfall. The rainfall predicted by the model for these days is mostly less than 1 mm and negligible in absolute terms. However, for such a pairwise comparison it tends to affect the outcome. A comparison of ERA5 rainfall and simulated rainfall for selected grid cells is shown in Figure S3.

3.2 | Impacts of historical deforestation on observed rainfall pattern

Historical deforestation in South America has substantially affected both local and regional rainfall patterns. As a result of cumulative effects, we find that the deforestation-induced changes in rainfall pattern are much more pronounced over recent years (2016–2020, which represent the last 5 years of the simulation period) than in earlier years. Hence, unless specified otherwise in this section, the changes in rainfall that we describe are for the 2016–2020 period. Over

deforestation hotspots delineated in this study, we find that the mean annual rainfall would have been 18% higher without the deforestation that occurred between 1982 and 2020 (Figure 5), and it would have been 10% higher without deforestation between 2000 and 2020 (Figure 6). Over areas not delineated as deforestation hotspots and where vegetation cover remained the same for all simulations, we find that the mean annual rainfall would have been 9% higher without deforestation in delineated hotspots between 1982 and 2020. It would have been 5% higher without deforestation between 2000 and 2020. These findings clearly show that deforestation does not only affect local rainfall but also rainfall in nearby or remote areas.

Much of the reduction in rainfall experienced due to deforestation is concentrated in the Amazon, Cerrado, and Caatinga biomes where substantial tree cover has been lost over the past four decades. For instance, in the Amazon biome, mean tree cover was reduced from about 82% in 1982 to less than 62% in 2020 (Figure 7a). As a result, 50% of the Amazon biome recorded a mean annual rainfall exceeding 1800 mm year^{-1} whereas, without recorded deforestation between 1982 and 2020, 75% of the Amazon biome would have exceeded this amount (Figure 7b). In the Cerrado, about 25% of the area recorded mean annual rainfall of exceeding 1300 mm year^{-1}, whereas without recorded deforestation between 1982 and 2020, 70% of the biome would have exceeded this amount.

We also find that historical deforestation has increased the relative entropy of rainfall especially in the Amazon–Cerrado frontier
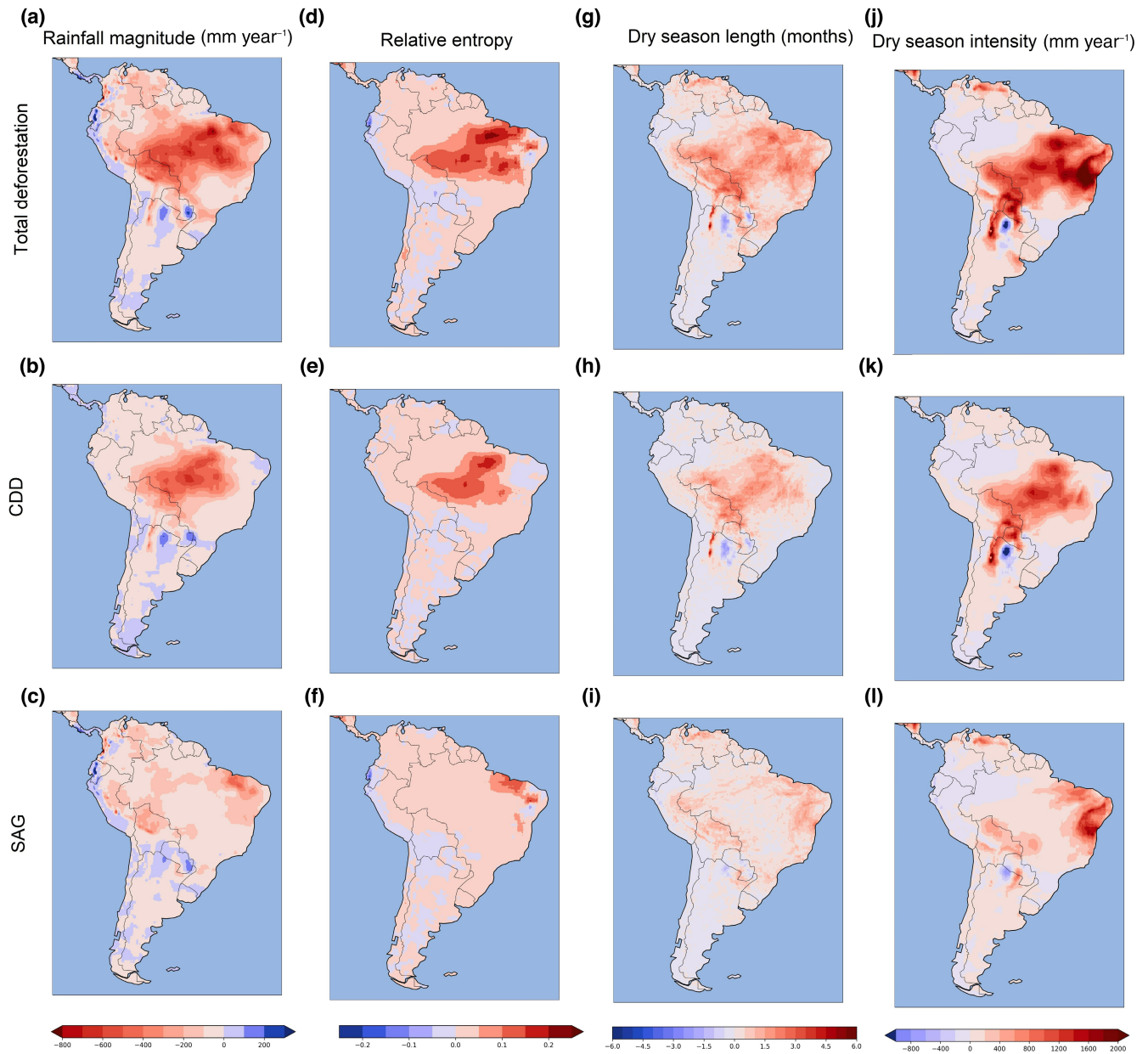
FIGURE 5 Changes in rainfall pattern averaged over the period 2016–2020 as a result of cumulative deforestation from 1982 to 2020. Estimated changes in rainfall magnitude (a–c); relative entropy (d–f); dry season length (g–i); and dry season intensity (j–l). Negative values indicate reduction as a result of deforestation and positive values indicate increase.

indicating that rainfall is concentrated in fewer months than would have been the case without historical deforestation (Figure 5d–f). Over the Amazon–Cerrado frontier, rainfall is concentrated in the November to May period. An increase in relative entropy indicates that without historical deforestation, rainfall magnitude would have been higher and would have been spread over more months than is currently the case. Over the Amazon biome, 40% of the area currently has a minimum relative entropy of 0.2 whereas without deforestation recorded between 1982 and 2020 this would have been 25% of the area (Figure 7c). In the Cerrado biome, 50% of the area currently has a minimum relative entropy of 0.4 whereas without deforestation between 1982 and 2020 this would have been 15% of

the area. Generally, because of cumulative effects, deforestation in the period 1982–2020 had greater negative impact on rainfall than in the period 2000–2020 (Figure 8).

To understand the societal impacts of deforestation-induced droughts or dry season changes, it is important to assess if the remaining rainfall is sufficient to satisfy crop or vegetation water demand. We used potential evapotranspiration as a measure of crop and vegetation water demand. Our findings show that dry season length, that is, the number of months when rainfall is less than potential evapotranspiration, has increased substantially over deforestation hotspots especially in the Amazon and the Cerrado and to a lesser extents over remote areas. Currently about 60% of the Amazon biome
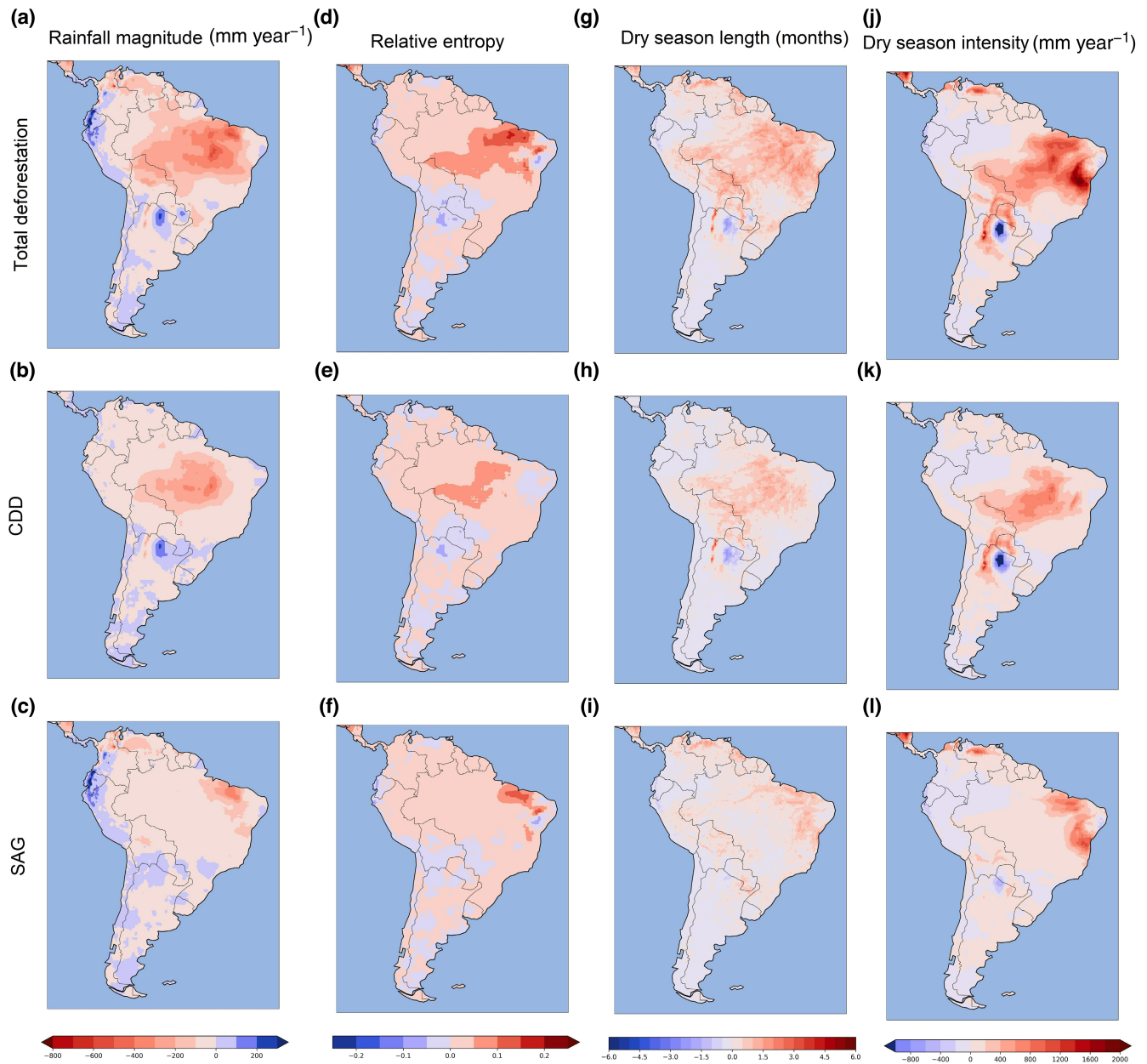
FIGURE 6 Changes in rainfall pattern averaged over the period 2016–2020 as a result of cumulative deforestation from 2000 to 2020. Estimated changes in rainfall magnitude (a–c); relative entropy (d–f); dry season length (g–i); and dry season intensity (j–l). Negative values indicate reduction as a result of deforestation and positive values indicate increase.

has at least 4 months where total precipitation is less than potential evapotranspiration. However, without deforestation between 1982 and 2020, this would have been only 25% of the area (Figures 5g–i and 7d). For the Cerrado, currently about 50% of the biome experience dry seasons of at least 7 months, whereas without deforestation only about 20% would have experienced a dry season of this duration (Figures 5g–i and 7d). Our findings also suggest that dry season duration has not only increased but, in addition, water deficit within these months have intensified (Figures 5j–l and 7e). Because potential evapotranspiration over a specific grid cell is unaffected by deforestation, increasing water deficit can be attributed to deforestation-induced changes in rainfall. We connected the change in rainfall to

the different drivers for deforestation based on Curtis et al. (2018), and found that the rainfall pattern changes revealed in our analysis have been caused largely by CDD whereas in the Caatinga it is driven largely by shifting agriculture (SAG) (Figures 5 and 6).

3.3 | Potential impacts of further deforestation on rainfall

Over the Amazon biome, the conversion of all forest cover outside protected areas to pasture would reduce rainfall magnitude substantially. Some areas would lose as much as 80% or more of annual
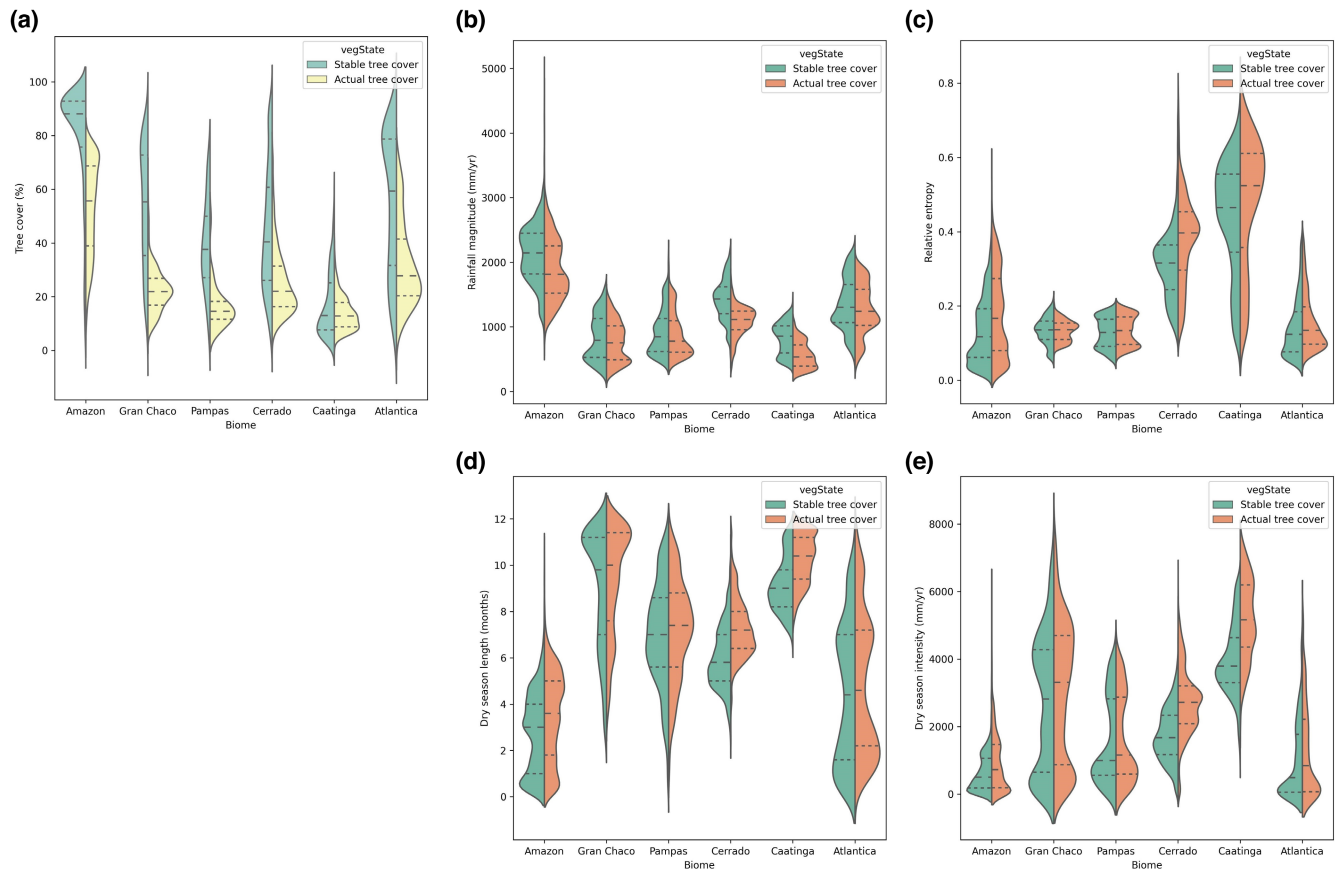
FIGURE 7 Probability distributions of tree cover and rainfall indices under actual and stable (year 1982) tree cover states in different biomes. Tree cover (a); rainfall magnitude (b); relative entropy (c); dry season length (d); and dry season duration (e). (b–e) were computed over the period 2016 to 2020.

rainfall (Figure 9). Over deforested areas, mean annual rainfall is likely to be reduced by about 48% in the Amazon biome whereas over non-deforested areas this would be 26%. Across the amazon biome, conversion of forest cover outside protected areas would reduce average annual rainfall by 36% and conversion of all forest cover including protected areas would reduce average annual rainfall by about 68%.

4 | DISCUSSION AND CONCLUSIONS

Our paper advances the current knowledge of forest–rainfall relationship by providing new quantitative insights on the rainfall effects of historical deforestation recorded over the past four decades and by disentangling the contribution of different drivers of deforestation to rainfall changes. The results show that historical deforestation has substantially reduced rainfall magnitude and increased dry season length and intensity especially in the Amazon, Cerrado, and Caatinga biomes. Our innovative data-driven modeling approach utilizes 20 years of tree cover and vegetation data. For the future deforestation scenarios that we apply in the Amazon, our results are in line with previous studies. For example, Sierra et al. (2022) find that further Amazonian

deforestation leading to 45% forest cover loss will result in a reduction in precipitation of about 20% over the entire Amazon basin, with the Southern part of the Amazon being most affected by reduced rainfall. We find that average annual rainfall in the Amazon would be reduced by 68% in the case of complete deforestation (i.e., conversion to pasture), and 36% in case of deforestation of all non-protected areas.

Despite our data-driven approach, uncertainties remain. In both analyses, the main uncertainty in our input dataset relates to the LAI and albedo data, which were unavailable for years before 2000 at the required temporal resolution. Therefore, we derived LAI and albedo curves for different tree cover intervals. Detailed dynamic LAI and albedo data used in the model development, to some extent capture effects of different tree and vegetation species on rainfall. But our use of generalized LAI and albedo profiles for different tree cover intervals in both our backward- and forward-looking analyses has the tendency to smoothen this phenomenon. The uncertainty related to the LAI and albedo of the vegetation replacing the forest in the future is of particular high relevance in the forward-looking analysis, because there is uncertainty on the type of land-use replacing forest cover. This differs across the Amazon, but typical land-use change involves selective logging of the forest, conversion to pasture and subsequently, over time, a gradual conversion
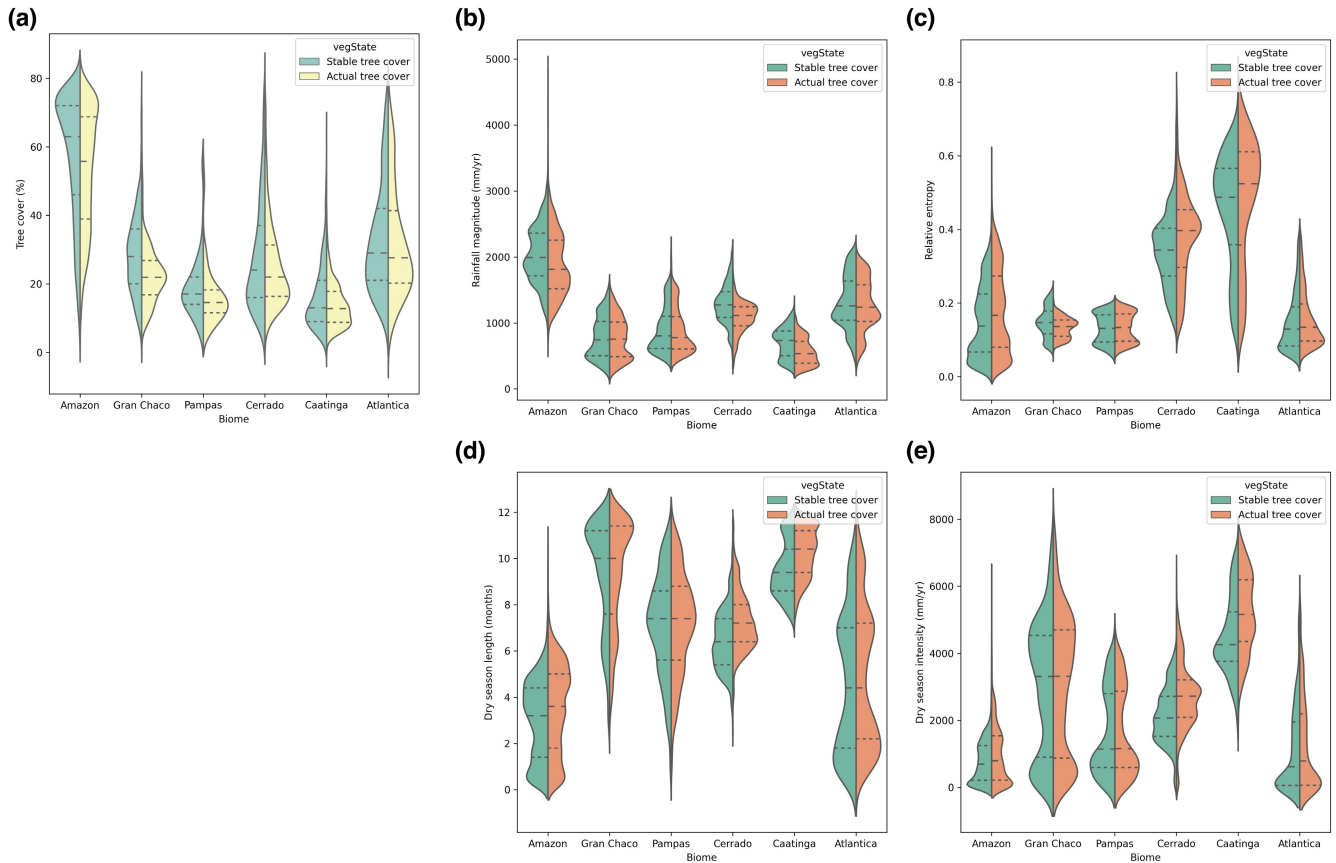
FIGURE 8 Probability distributions of tree cover and rainfall indices under actual and stable (year 2000) tree cover states. Tree cover (a); rainfall magnitude (b); relative entropy (c); dry season length (d); and dry season duration (e). (b–e) were computed over the period 2016 to 2020.

FIGURE 9 Relative changes (%) in rainfall magnitude as a result of the conversion of tree cover outside protected areas in the Amazon biome (green boundary) to pasture (a); and all tree cover in the biome to pasture (b). Negative values indicate reduction in rainfall as a result of deforestation and positive values indicate increase.
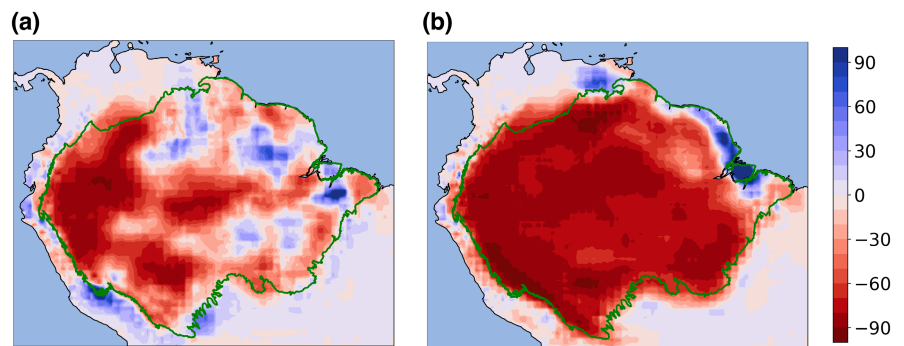
to soybean crops (Song et al., 2021). Our forward-looking analysis involves extreme scenarios, nonetheless, they relate to a scenario in which policy choices are made supporting the large-scale conversion of forests to agricultural use—a process that has been ongoing in Brazil in the agricultural frontier states of Bahia, Maranhão, Piaui, and Tocantins (Coe et al., 2017). Brazilian law protects forests, however, enforcement is a challenge and land conversion is still ongoing (Mataveli et al., 2022). As a result, from 1985 to 2021 the area dedicated to croplands and pasture increased by 86 million hectares, mainly in the agricultural frontier states of Mato Grosso, Goias, Bahia, Maranhao, Piaui, and Tocantins (Souza et al., 2020).

Given that the loss of forests has been rapid (and accelerating since 2015 (INPE, 2022; Mataveli et al., 2022)), the government of Brazil and other stakeholders in the country need to decide what level of protection to confer to the forests outside of protected areas.

We note that impacts of future deforestation are, in particular, prone to uncertainty including from threshold effects in ecosystem responses (e.g., Ratajczak et al., 2018). A number of studies with global climate models that incorporate various levels of deforestation suggest that tropical forest clearing beyond ~30%–50% may constitute a critical threshold for the Amazon, beyond which reduced rainfall triggers a significant decline in ecosystem structure

and function (Lawrence & Vandecar, 2015). Even though our study confirms that major changes in rainfall magnitude and dry season length are likely to occur in case large areas would be deforested, we did not investigate the specific threshold below which deforestation in the Amazon leads to an abrupt change in rainfall. We note that there are several other feedback mechanisms in the ecosystem that we did not include in our model and that could accelerate rainfall changes compared to our model outcomes. For instance, reduced rainfall may increase fire risks (Hoffmann et al., 2003; Holden et al., 2018) that may cause further reductions in forest cover. Since we do not consider such feedbacks in our analysis, we may underestimate the effects of deforestation on rainfall patterns. We also note that such dynamics may be subject to hysteresis, that is, restoring rainfall patterns may well require forest cover to be restored to a higher density compared to the threshold where threshold effects first occurred.

Our findings clearly show past deforestation has negatively affected rainfall patterns over deforested areas as well as non-deforested areas especially in the Amazon–Cerrado agricultural frontier. These changes in rainfall patterns have had and will continue to have severe agronomic and economic implications that urgently need to be acknowledged in agrobusinesses and in policy making. Reductions in rainfall immediately impact agricultural yields given that rainfall is already a major constraint to agricultural productivity in parts of the Amazon and much of the Cerrado biome (e.g., Lawrence & Vandecar, 2015; Leite-Filho et al., 2021). Hence, there is a critical trade-off at play. Converting forest to cropland and pastures increases land available for agriculture, but at the same time reduces yields across existing and new croplands and pastures. This trade-off is not yet well understood, and there is an urgent need for further work to inform policy making how far Brazil is removed from the point where converting additional land to cropland and pastures actually reduces economic outputs. These effects will not be uniformly spread across the Amazon: our findings show that the relative impacts on rainfall are highest in the Southern arch of the Amazon (see Figures 5 and 6), yet the impacts on crop production may be highest in areas with currently a low rainfall compared to the needs of the main crops, in particular Bahia state. Furthermore, policy making should consider that the forest–rainfall relationship is prone to uncertainty and that critical thresholds exist which, together with teleconnection effects, may cause the rainfall system to collapse quicker than is indicated by the current projections.

CONFLICT OF INTEREST STATEMENT

The authors have no conflicts of interest to declare.

DATA AVAILABILITY STATEMENT

The data that support the findings of this study are openly available in Zenodo at https://doi.org/10.5281/zenodo.8071547.

ORCID

Confidence Duku https://orcid.org/0000-0002-1670-3451

REFERENCES

Abatzoglou, J. T., Dobrowski, S. Z., Parks, S. A., & Hegewisch, K. C. (2018). TerraClimate, a high-resolution global dataset of monthly climate and climatic water balance from 1958–2015. *Scientific Data*, 5(1), 170191. https://doi.org/10.1038/sdata.2017.191

Allen, R. G., Pereira, L. S., Raes, D., & Smith, M. (1998). *Crop evapotranspiration-guidelines for computing crop water requirements-FAO Irrigation and Drainage Paper 56*. FAO, 300(9), D05109.

Amigo, I. (2020). When will the Amazon hit a tipping point? *Nature*, 578(7796), 505–508.

Aragão, L. E. O. C., Malhi, Y., Roman-Cuesta, R. M., Saatchi, S., Anderson, L. O., & Shimabukuro, Y. E. (2007). Spatial patterns and fire response of recent Amazonian droughts. *Geophysical Research Letters*, 34(7), L07701. https://doi.org/10.1029/2006GL028946

Coe, M. T., Brando, P. M., Deegan, L. A., Macedo, M. N., Neill, C., & Silvério, D. V. (2017). The forests of the Amazon and Cerrado moderate regional climate and are the key to the future. *Tropical Conservation Science*, 10, 1940082917720671. https://doi.org/10.1177/1940082917720671

Cui, J., Lian, X., Huntingford, C., Gimeno, L., Wang, T., Ding, J., He, M., Xu, H., Chen, A., Gentine, P., & Piao, S. (2022). Global water availability boosted by vegetation-driven changes in atmospheric moisture transport. *Nature Geoscience*, 15(12), 982–988. https://doi.org/10.1038/s41561-022-01061-7

Curtis, P. G., Slay, C. M., Harris, N. L., Tyukavina, A., & Hansen, M. C. (2018). Classifying drivers of global forest loss. *Science*, 361(6407), 1108–1111. https://doi.org/10.1126/science.aau3445

DiMiceli, C., Townshend, J., Carroll, M., & Sohlberg, R. (2021). Evolution of the representation of global vegetation by vegetation continuous fields. *Remote Sensing of Environment*, 254, 112271. https://doi.org/10.1016/j.rse.2020.112271

Duku, C., & Hein, L. (2021). The impact of deforestation on rainfall in Africa: A data-driven assessment. *Environmental Research Letters*, 16(6), 064044. https://doi.org/10.1088/1748-9326/abfcfb

Ellison, D., Morris, C. E., Locatelli, B., Sheil, D., Cohen, J., Murdiyarso, D., Gutierrez, V., Noordwijk, M. V., Creed, I. F., Pokorny, J., Gaveau, D., Spracklen, D. V., Tobella, A. B., Ilstedt, U., Teuling, A. J., Gebrehiwot, S. G., Sands, D. C., Muys, B., Verbist, B., ... Sullivan, C. A. (2017). Trees, forests and water: Cool insights for a hot world. *Global Environmental Change*, 43, 51–61. https://doi.org/10.1016/j.gloenvcha.2017.01.002

Feng, X., Porporato, A., & Rodriguez-Iturbe, I. (2013). Changes in rainfall seasonality in the tropics. *Nature Climate Change*, 3(9), 811–815. https://doi.org/10.1038/nclimate1907

Hersbach, H., Bell, B., Berrisford, P., Hirahara, S., Horányi, A., Muñoz-Sabater, J., Nicolas, J., Peubey, C., Radu, R., Schepers, D., Simmons, A., Soci, C., Abdalla, S., Abellan, X., Balsamo, G., Bechtold, P., Biavati, G., Bidlot, J., Bonavita, M., ... Thépaut, J.-N. (2020). The ERA5 global reanalysis. *Quarterly Journal of the Royal Meteorological Society*, 146(730), 1999–2049. https://doi.org/10.1002/qj.3803

Hoffmann, W. A., Schroeder, W., & Jackson, R. B. (2003). Regional feedbacks among fire, climate, and tropical deforestation. *Journal of Geophysical Research: Atmospheres*, 108(D23), 4721. https://doi.org/10.1029/2003JD003494

Holden, Z. A., Swanson, A., Luce, C. H., Jolly, W. M., Maneta, M., Oyler, J. W., Warren, D. A., Parsons, R., & Affleck, D. (2018). Decreasing fire season precipitation increased recent western US forest wildfire activity. *Proceedings of the National Academy of Sciences of the United States of America*, 115(36), E8349–E8357. https://doi.org/10.1073/pnas.1802316115

INPE. (2022). *PRODES—Monitoramento da Floresta Amazônica Brasileira por Satélite. INPE databaseTerraBrasilis (INPE.br)*. http://terrabrasilis.dpi.inpe.br/app/dashboard/deforestation/biomes/amazon/increments

Kalamandeen, M., Gloor, E., Mitchard, E., Quincey, D., Ziv, G., Spracklen, D., Spracklen, B., Adami, M., Aragão, L. E. O. C., & Galbraith, D. (2018).

Pervasive rise of small-scale deforestation in Amazonia. *Scientific Reports*, 8(1), 1600. https://doi.org/10.1038/s41598-018-19358-2

Khanna, J., Medvigy, D., Fueglistaler, S., & Walko, R. (2017). Regional dry-season climate changes due to three decades of Amazonian deforestation. *Nature Climate Change*, 7(3), 200–204. https://doi.org/10.1038/nclimate3226

Konapala, G., Mishra, A. K., Wada, Y., & Mann, M. E. (2020). Climate change will affect global water availability through compounding changes in seasonal precipitation and evaporation. *Nature Communications*, 11(1), 3044. https://doi.org/10.1038/s41467-020-16757-w

Lawrence, D., & Vandecar, K. (2015). Effects of tropical deforestation on climate and agriculture. *Nature Climate Change*, 5(1), 27–36. https://doi.org/10.1038/nclimate2430

Leite-Filho, A. T., Soares-Filho, B. S., Davis, J. L., Abrahão, G. M., & Börner, J. (2021). Deforestation reduces rainfall and agricultural revenues in the Brazilian Amazon. *Nature Communications*, 12(1), 2591. https://doi.org/10.1038/s41467-021-22840-7

Masson-Delmotte, V., Zhai, P., Pirani, A., Connors, S. L., Péan, C., Berger, S., Caud, N., Chen, Y., Goldfarb, L., & Gomis, M. (2021). Climate change 2021: The physical science basis. *Contribution of Working Group I to the Sixth Assessment Report of the Intergovernmental Panel on Climate Change*, 2.

Mataveli, G., de Oliveira, G., Chaves, M. E., Dalagnol, R., Wagner, F. H., Ipia, A. H., Silva-Junior, C. H., & Aragão, L. E. (2022). Science-based planning can support law enforcement actions to curb deforestation in the Brazilian Amazon. *Conservation Letters*, 15, e12908.

Meier, R., Schwaab, J., Seneviratne, S. I., Sprenger, M., Lewis, E., & Davin, E. L. (2021). Empirical estimate of forestation-induced precipitation changes in Europe. *Nature Geoscience*, 14(7), 473–478. https://doi.org/10.1038/s41561-021-00773-6

Myneni, R., Knyazikhin, Y., & Park, T. (2015). *MCD15A3H MODIS/Terra+Aqua Leaf Area Index/FPAR 4-day L4 Global 500m SIN Grid V006.* https://doi.org/10.5067/MODIS/MCD15A3H.006

Ratajczak, Z., Carpenter, S. R., Ives, A. R., Kucharik, C. J., Ramiadantsoa, T., Stegner, M. A., Williams, J. W., Zhang, J., & Turner, M. G. (2018). Abrupt change in ecological systems: Inference and diagnosis. *Trends in Ecology & Evolution*, 33(7), 513–526. https://doi.org/10.1016/j.tree.2018.04.013

Reynolds, R., & Banzon, V. (2008). NOAA optimum interpolation 1/4 degree daily sea surface temperature (OISST) analysis, version 2. *NOAA National Centers for Environmental Information*, 10, V5SQ8XB5.

Salazar, A., Baldi, G., Hirota, M., Syktus, J., & McAlpine, C. (2015). Land use and land cover change impacts on the regional climate of non-Amazonian South America: A review. *Global and Planetary Change*, 128, 103–119. https://doi.org/10.1016/j.gloplacha.2015.02.009

Schaaf, C., & Wang, Z. (2015). *MCD43D51 MODIS/Terra+aqua BRDF/albedo black sky albedo shortwave daily L3 global 30arcsec CMG V006.* https://doi.org/10.5067/MODIS/MCD43D51.006

Shi, X., Chen, Z., Wang, H., Yeung, D.-Y., Wong, W.-K., & Woo, W.-C. (2015). Convolutional LSTM network: A machine learning approach for precipitation nowcasting *(Montreal, Canada) 29th Annual Conference on Neural Information Processing Systems, NIPS 2015*.

Sierra, J. P., Junquas, C., Espinoza, J. C., Segura, H., Condom, T., Andrade, M., Molina-Carpio, J., Ticona, L., Mardoñez, V., Blacutt, L., Polcher, J., Rabatel, A., & Sicart, J. E. (2022). Deforestation impacts on Amazon-Andes hydroclimatic connectivity. *Climate Dynamics*, 58(9), 2609–2636. https://doi.org/10.1007/s00382-021-06025-y

Smith, C., Baker, J. C. A., & Spracklen, D. V. (2023). Tropical deforestation causes large reductions in observed precipitation. *Nature*, 615(7951), 270–275. https://doi.org/10.1038/s41586-022-05690-1

Song, X.-P., Hansen, M. C., Potapov, P., Adusei, B., Pickering, J., Adami, M., Lima, A., Zalles, V., Stehman, S. V., Di Bella, C. M., Conde, M. C., Copati, E. J., Fernandes, L. B., Hernandez-Serna, A., Jantz, S. M., Pickens, A. H., Turubanova, S., & Tyukavina, A. (2021). Massive soybean expansion in South America since 2000 and implications for conservation. *Nature Sustainability*, 4(9), 784–792. https://doi.org/10.1038/s41893-021-00729-z

Souza, C. M., Shimbo, J. Z., Rosa, M. R., Parente, L., Alencar, A. A., Rudorff, B. F. T., Hasenack, H., Matsumoto, M., Ferreira, L. G., Souza-Filho, P. W. M., de Oliveira, S. W., Rocha, W. F., Fonseca, A. V., Marques, C. B., Diniz, C. G., Costa, D., Monteiro, D., Rosa, E. R., Vélez-Martin, E., … Azevedo, T. (2020). Reconstructing three decades of land use and land cover changes in Brazilian biomes with Landsat archive and earth engine. *Remote Sensing*, 12(17), 2735 https://www.mdpi.com/2072-4292/12/17/2735

Spracklen, D. V., Baker, J. C. A., Garcia-Carreras, L., & Marsham, J. H. (2018). The effects of tropical vegetation on rainfall. *Annual Review of Environment and Resources*, 43(1), 193–218. https://doi.org/10.1146/annurev-environ-102017-030136

Spracklen, D. V., & Garcia-Carreras, L. (2015). The impact of Amazonian deforestation on Amazon basin rainfall. *Geophysical Research Letters*, 42(21), 9546–9552. https://doi.org/10.1002/2015GL066063

Staal, A., Fetzer, I., Wang-Erlandsson, L., Bosmans, J. H. C., Dekker, S. C., van Nes, E. H., Rockström, J., & Tuinenburg, O. A. (2020). Hysteresis of tropical forests in the 21st century. *Nature Communications*, 11(1), 4978. https://doi.org/10.1038/s41467-020-18728-7

Staal, A., Flores, B. M., Aguiar, A. P. D., Bosmans, J. H. C., Fetzer, I., & Tuinenburg, O. A. (2020). Feedback between drought and deforestation in the Amazon. *Environmental Research Letters*, 15(4), 044024. https://doi.org/10.1088/1748-9326/ab738e

Staal, A., Tuinenburg, O. A., Bosmans, J. H. C., Holmgren, M., van Nes, E. H., Scheffer, M., Zemp, D. C., & Dekker, S. C. (2018). Forest-rainfall cascades buffer against drought across the Amazon. *Nature Climate Change*, 8(6), 539–543. https://doi.org/10.1038/s41558-018-0177-y

te Wierik, S. A., Cammeraat, E. L. H., Gupta, J., & Artzy-Randrup, Y. A. (2021). Reviewing the impact of land use and land-use change on moisture recycling and precipitation patterns. *Water Resources Research*, 57(7), e2020WR029234. https://doi.org/10.1029/2020WR029234

UNEP-WCMC, & IUCN. (2022). *Protected planet: The World Database on Protected Areas (WDPA).*

Virtanen, P., Gommers, R., Oliphant, T. E., Haberland, M., Reddy, T., Cournapeau, D., Burovski, E., Peterson, P., Weckesser, W., Bright, J., van der Walt, S. J., Brett, M., Wilson, J., Millman, K. J., Mayorov, N., Nelson, A. R. J., Jones, E., Kern, R., Larson, E., … SciPy 1.0 Contributors. (2020). SciPy 1.0: Fundamental algorithms for scientific computing in Python. *Nature Methods*, 17(3), 261–272. https://doi.org/10.1038/s41592-019-0686-2

SUPPORTING INFORMATION

Additional supporting information can be found online in the Supporting Information section at the end of this article.

How to cite this article: Duku, C., & Hein, L. (2023). Assessing the impacts of past and ongoing deforestation on rainfall patterns in South America. *Global Change Biology, 29*, 5292–5303. https://doi.org/10.1111/gcb.16856